ISSN 1674-1056
http://cpb.iphy.ac.cn
http://iopscience.iop.org/cpb
中国物理 B
Chinese Physics
中国物理 Chinese Physics B

Effects of buried oxide layer on working speed of SiGe heterojunction photo-transistor

Xian-Cheng Liu(刘先程), Jia-Jun Ma(马佳俊), Hong-Yun Xie(谢红云), Pei Ma(马佩), Liang Chen(陈亮), Min Guo(郭敏), Wan-Rong Zhang(张万荣)
Citation: Chin. Phys. B . 2020, 29(2): 028501 . **doi:** 10.1088/1674-1056/ab5f01
Journal homepage: http://cpb.iphy.ac.cn; http://iopscience.iop.org/cpb

What follows is a list of articles you may be interested in

High performance silicon-based GeSn p-i-n photodetectors for short-wave infrared application

Yue Zhao(赵越), Nan Wang(王楠), Kai Yu(余凯), Xiaoming Zhang(张晓明), Xiuli Li(李秀丽), Jun Zheng(郑军), Chunlai Xue(薛春来), Buwen Cheng(成步文), Chuanbo Li(李传波)
Chin. Phys. B . 2019, 28(12): 128501 . **doi:** 10.1088/1674-1056/ab4e84

The origin of distorted intensity pattern sensed by a lens and antenna coupled AlGaN/GaN-HEMT terahertz detector

Xiang Li(李想)[1,2], Jian-Dong Sun(孙建东)[1], Hong-Juan Huang(黄宏娟)[3], Zhi-Peng Zhang(张志鹏)[1], Lin Jin(靳琳)[1], Yun-Fei Sun(孙云飞)[4], V V Popov[5], Hua Qin(秦华)[1]
Chin. Phys. B . 2019, 28(11): 118502 . **doi:** 10.1088/1674-1056/ab44ac

Influence of characteristics' measurement sequence on total ionizing dose effect in PDSOI nMOSFET

Xin Xie(解鑫), Da-Wei Bi(毕大伟), Zhi-Yuan Hu(胡志远), Hui-Long Zhu(朱慧龙), Meng-Ying Zhang(张梦映), Zheng-Xuan Zhang(张正选), Shi-Chang Zou(邹世昌)
Chin. Phys. B . 2018, 27(12): 128501 . **doi:** 10.1088/1674-1056/27/12/128501

Fabrication and characterization of novel high-speed InGaAs/InP uni-traveling-carrier photodetector for high responsivity

Chen Qing-Tao, Huang Yong-Qing, Fei Jia-Rui, Duan Xiao-Feng, Liu Kai, Liu Feng, Kang Chao, Wang Jun-Chu, Fang Wen-Jing, Ren Xiao-Min
Chin. Phys. B . 2015, 24(10): 108506 . **doi:** 10.1088/1674-1056/24/10/108506

Effects of back gate bias on radio-frequency performance in partially depleted silicon-on-inslator nMOSFETs

Lü Kai, Chen Jing, Luo Jie-Xin, He Wei-Wei, Huang Jian-Qiang, Chai Zhan, Wang Xi
Chin. Phys. B . 2015, 24(8): 088501 . **doi:** 10.1088/1674-1056/24/8/088501

Effects of buried oxide layer on working speed of SiGe heterojunction photo-transistor*

Xian-Cheng Liu(刘先程)[1], Jia-Jun Ma(马佳俊)[1], Hong-Yun Xie(谢红云)[1,†], Pei Ma(马佩)[1], Liang Chen(陈亮)[2], Min Guo(郭敏)[1], and Wan-Rong Zhang(张万荣)[1]

[1] *Faculty of Information Technology, Beijing University of Technology, Beijing* 100124, *China*
[2] *College of Physics and Electronic Engineering, Taishan University, Taian* 271000, *China*

(Received 21 August 2019; revised manuscript received 21 November 2019; accepted manuscript online 5 December 2019)

The effects of buried oxide (BOX) layer on the capacitance of SiGe heterojunction photo-transistor (HPT), including the collector–substrate capacitance, the base–collector capacitance, and the base–emitter capacitance, are studied by using a silicon-on-insulator (SOI) substrate as compared with the devices on native Si substrates. By introducing the BOX layer into Si-based SiGe HPT, the maximum photo-characteristic frequency $f_{t,opt}$ of SOI-based SiGe HPT reaches up to 24.51 GHz, which is 1.5 times higher than the value obtained from Si-based SiGe HPT. In addition, the maximum optical cut-off frequency $f_{\beta,opt}$, namely its 3-dB bandwidth, reaches up to 1.13 GHz, improved by 1.18 times. However, with the increase of optical power or collector current, this improvement on the frequency characteristic from BOX layer becomes less dominant as confirmed by reducing the 3-dB bandwidth of SOI-based SiGe HPT which approaches to the 3-dB bandwidth of Si-based SiGe HPT at higher injection conditions.

Keywords: silicon-on-insulator (SOI), SiGe heterojunction photo-transistor (HPT), characteristic frequency, 3-dB bandwidth

PACS: 85.60.Gz, 85.60.Bt, 78.66.Nk, 73.40.Lq **DOI:** 10.1088/1674-1056/ab5f01

1. Introduction

In recent years, optical information transmission technology is a growing area of research interest for developing the high-speed telecommunications and data exchange and computing. In the fields of optical communication, optical interconnection and other relative fields, there have been growing the demands for high performance components and modules.[1,2] As one of the core components, the photodetector plays a decisive role in the whole system.[3] At present, vertical Si-based SiGe heterojunction photo-transistor (HPT), one of the important optical receivers, possesses a variety of advantages such as low power consumption, low cost and high compatibility with complementary metal–oxide–semiconductor (CMOS) technology.[4–6] Recently, research interest turned to improving the responsivity and working speed of SiGe HPT. However, due to the existence of junction capacitance and the slow-photon-generated carriers in the Si substrate, the working speed of the device is greatly limited.[7–11]

To improve the working speed of the Si-based SiGe HPT, a buried oxide (BOX) layer is introduced into its collector in this paper. Due to the existence of series capacitance of BOX layer, the collector–substrate capacitance, the base–collector junction capacitance as well as the base–emitter junction capacitance are reduced to a certain degree. Moreover, the BOX layer will isolate the slow carriers in the silicon substrate. Therefore the working speed of SOI-based SiGe HPT is predicted to be faster than that of SiGe HPT on native Si substrates.

2. Device structure

Figure 1 shows the structure of an SOI-based SiGe HPT (Fig. 1(a)). The structure of a common Si-based SiGe HPT (Fig. 1(b)) is also shown in Fig. 1. The epitaxial structure comes from the common Si-based SiGe HPT with a full area emitter and a 20 μm×20 μm optical window, which was presented by Rosales *et al.*[7] The Si-based SiGe HPT presented here was implemented by using an 80-GHz SiGe bipolar process technology, and an extracted 3-dB bandwidth of 728 MHz was achieved.[5] The SOI substrate was realized with the implanted oxygen (SIMOX) technology, and the p^+-type SiGe base is epitaxially grown with ultrahigh vacuum chemical vapor deposition (UHV-CVD) technology. The epitaxial structure is composed of a 300-nm BOX layer, a 300-nm n^+-type sub-collector with high doping (2×10^{19} cm^{-3}), a 600-nm n^--type collector with low doping (7×10^{16} cm^{-3}), an 80-nm high doping (1×10^{19} cm^{-3}) p^+-type $Si_{0.8}Ge_{0.2}$ base, and finally a 300-nm n^+-type polysilicon emitter with high doping (2×10^{20} cm^{-3}), fabricated with low pressure chemical vapor deposition (LPCVD) technology. Clearly, the only difference

*Project supported by the National Natural Science Foundation of China (Grant Nos. 61604106, 61774012, and 61901010), the Beijing Future Chip Technology High Precision Innovation Center Research Fund, China (Grant No. KYJJ2016008), the Beijing Municipal Natural Science Foundation, China (Grant No. 4192014), and the Municipal Natural Science Foundation of Shangdong Province, China (Grant No. ZR2014FL025).

†Corresponding author. E-mail: xiehongyun@bjut.edu.cn

© 2020 Chinese Physical Society and IOP Publishing Ltd

between these two devices lies in the BOX layer between the sub-collector and the substrate. The effect of BOX layer on the SiGe HPT is discussed in the following section in detail.

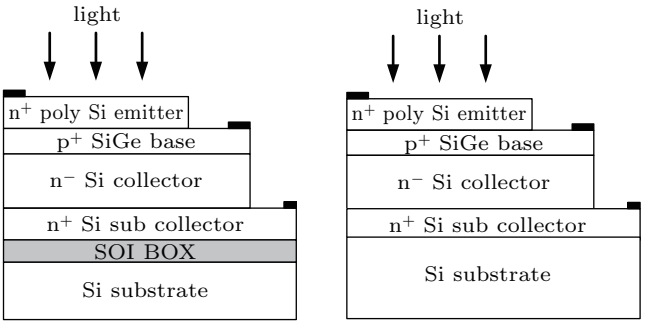


Fig. 1. Device structures of SiGe HPT. (a) SOI-based and (b) Si-based.

3. Results and discussion

3.1. Collector–substrate capacitance

Figure 2 shows the plots of collector–substrate capacitance C_{cs} of SiGe HPT under different collector currents for two devices, respectively. It is obvious that the C_{cs} of SOI-based SiGe HPT is always smaller than that of Si-based SiGe HPT. The maximum value of C_{cs} of SOI-based SiGe HPT and of Si-based SiGe HPT are 0.34 fF and 9.23 fF respectively, and the maximum capacitance is suppressed by 96.32%.

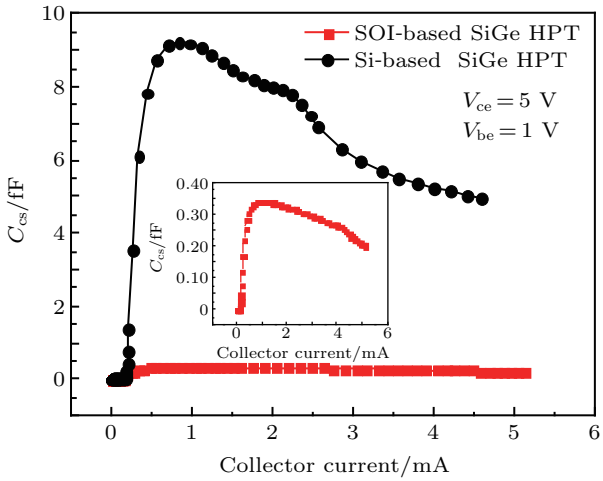


Fig. 2. Plot of C_{cs} *versus* collector current for SOI-based SiGe HPT and for Si-based SiGe HPT.

For SOI-based SiGe HPT, the collector–substrate capacitor C_{cs} is composed of BOX capacitor C_{ox} and BOX-substrate capacitor C_{cs-sub}. These two capacitors are in series connection electrically and so the total capacitance of C_{cs} must be smaller than that of either of them. Meanwhile, the C_{cs} of Si-based SiGe HPT is only the collector–substrate capacitance and it will be larger than the total series capacitance of the SOI-based SiGe HPT.

For an SOI-based SiGe HBT, the introduction of the BOX layer will reduce the electron concentration of the sub collector near the BOX layer and then results in a bigger sub-collector resistance.[12] The electron concentration in sub-collector of SOI-based SiGe HBT, SOI-based SiGe HPT and Si-based SiGe HPT are shown in Fig. 3. The electron concentration of the SOI-based SiGe HPT near the Si/SiO_2 interface is at the same level as that of the collector section and higher than those of the SOI-based SiGe HBT and the Si-based SiGe HPT. For an SOI-based SiGe HPT, the presence of BOX layer is beneficial for recycling transmission light back to the absorption layer because of the difference in index between Si sub-collector and BOX layer. This is equivalent to extending the absorption length, and thus improving the light absorption efficiency.[13] Thus, unlike an SOI-based SiGe HBT, the BOX layer introduced into SiGe HPT does not reduce the electron concentration obviously. Therefore, the resistance of the sub-collector in the SOI-based SiGe HPT is almost unchanged or slightly increased.

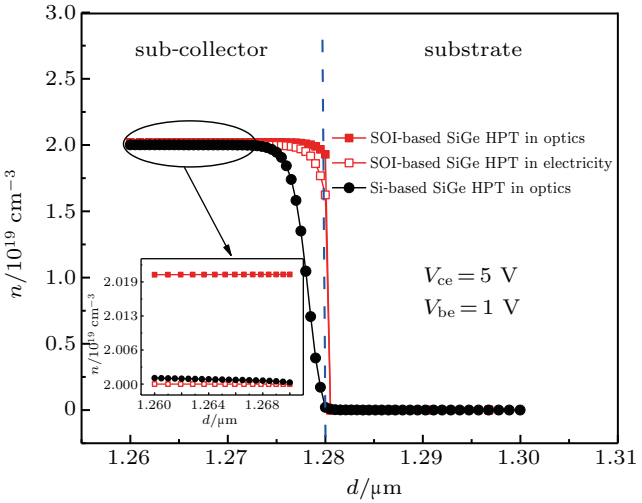


Fig. 3. Electron concentration distribution in vertical direction of sub collector.

3.2. Base–collector capacitance

Figure 4 shows the curves of the base–collector capacitance C_{bc} of SiGe HPT under different collector currents for two devices respectively. It is observed that with the introduction of BOX layer, when the collector current is less than 1.5 mA, the C_{bc} of SOI-based SiGe HPT is lower than that of Si-based SiGe HPT. The maximum value of C_{bc} decreases from 7.0 pF to 5.72 pF, a reduction of 18.29%. With the increase of collector current, the C_{bc} of SOI-based SiGe HPT is slightly higher than that of Si-based SiGe HPT.

The base–collector capacitance C_{bc} consists of barrier capacitance C_{TC} and diffusion capacitance C_{DC}. As the base–collector of SiGe HPT works at reverse bias, the diffusion capacitance C_{DC} can be ignored. Therefore only the barrier capacitance needs considering. The barrier capacitance C_{TC} can be expressed as[14]

$$C_{TC}=A_{j,BC}\left(\frac{q\varepsilon_{Si}}{2(V_{bi}-V_{BC}-V_{BC,opt})}\frac{N_B N_C}{N_B+N_C}\right)^{1/2}, \quad (1)$$

where V_{bi} is the built-in voltage of space charge region, V_{bc} is the applied voltage, N_B and N_C are the doping concentration in base region and collector region respectively, and $V_{bc.opt}$ is the photo-generated voltage of base–collector.

As the HPT device is exposed to light incidence, there are photon-generated carriers in the collector region. Because of the low mobility of holes, photon-generated holes accumulate at the interface of collector depletion region, which induces the space charge effect, especially under high collector current.[15] Thus the photon-generated voltage of base–collector $V_{bc.opt}$ increases, causing the value of C_{bc} to increase.

As described above, the presence of BOX layer is beneficial to improving the light absorption efficiency. Then, SOI-based SiGe HPT will generate more photon-generated holes in collector region than Si-based SiGe HPT, the space charge effect of SOI-based SiGe HPT is more serious than that of Si-based SiGe HPT. Thus, as shown in Fig. 4, when the collector current is larger than 1.5 mA, the C_{bc} of SOI-based SiGe HPT is slightly higher than that of Si-based SiGe HPT.

For the reduction of C_{bc} in SOI-based SiGe HPT at low collector current, the serial BOX layer capacitance C_{ox} should be considered. When the collector current is low, the hole accumulation at the interface of depletion region of collector is small and the space charge effect is not significant. From Fig. 4 we can derive that the existence of series capacitors of BOX layer C_{ox} become dominated and has a bigger effect on base–collector capacitance at low collector current. Because of the series connection electrically, the BOX layer capacitance C_{ox} makes the total base–collector capacitance C_{bc} decrease, as shown in Fig. 4 when the collector current is smaller than 1.5 mA.

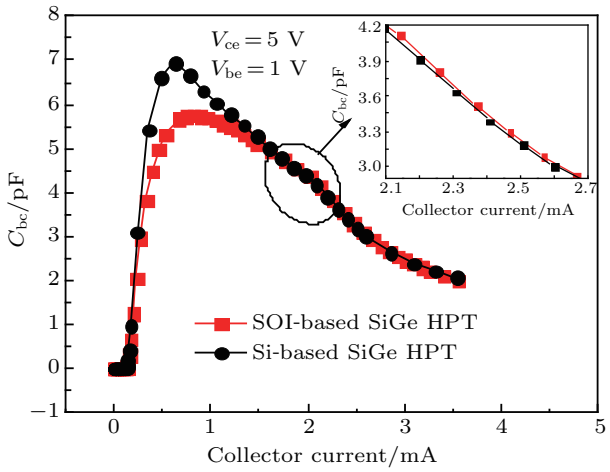


Fig. 4. Curve of C_{bc} *versus* collector current for SOI-based SiGe HPT and for Si-based SiGe HPT.

3.3. Base–emitter capacitance

The base–emitter capacitance C_{be} consists of barrier capacitance C_{TE} and diffusion capacitance C_{DE}. As the built-in voltage of space charge region V_{bi} is about 1.1 V, which is close to the applied voltage V_{BE} of 1 V in normal operation, only the diffusion capacitance C_{DE} needs considering. The C_{DE} can be expressed as[16]

$$C_{DE} = A_{j,BE}\frac{q^2}{KT}\left(p_{n0}L_p + n_{p0}L_n\right)\mathrm{e}^{q(V_{BE,opt}+V_{BE})/KT}, \quad (2)$$

where p_{n0} and n_{p0} are the minority carrier concentration in the emitter region and base region respectively, L_p and L_n are the hole diffusion length and electron diffusion length, respectively.

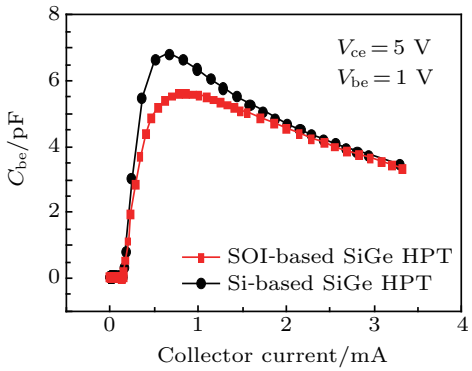


Fig. 5. Curve of C_{be} *versus* collector current for SOI-based SiGe HPT and for Si-based SiGe HPT.

Figure 5 shows the curves for base–emitter capacitance C_{be} of SiGe HPT under different collector currents for two devices, respectively. It is observed that the base–emitter capacitance C_{be} of SOI-based SiGe HPT is smaller than that of Si-based SiGe HPT. At low current, the maximum value of C_{be} decreases from 6.85 pF to 5.62 pF, a reduction of 17.96%. When the current increases, although the C_{be} of Si-based SiGe HPT decreases faster than the SOI-based HPT, the C_{be} of SOI-based SiGe HPT is still smaller in the operation current range.

After introducing BOX layer into Si-based SiGe HPT, there are always a lot interface states at Si/SiO_2 interface and many trap charges in BOX layer. Both become the recombination centers and then increase the recombination rate of carriers, reduce their lifetimes and further reduce their diffusion lengths. As a consequence, the SOI-based SiGe HPT has more recombination centers and the carrier diffusion length is shorter than the Si-based SiGe HPT. Therefore, the base–emitter diffusion capacitance of SOI-based SiGe HPT is always smaller than that of Si-based SiGe HPT.

3.4. Photo-characteristic frequency and 3-dB bandwidth

To analyze the frequency performance of SOI-based SiGe HPT, a two-dimensional (2D) simulation model is built with TCAD software Silvaco. The basic semiconductor equations, including Poisson equation, carrier continuity equation and carrier transport equation, are solved with Newton iteration and Gummel iteration through simulations. In this model, the mobility model consists of concentration-dependent mobility (conmob) model and parallel electric field-dependent mobility (fldmob) model. Considered in the recombination

model are the optical recombination, the Auger recombination, the Shockley–Read–Hall (SRH) recombination, as well as trap and surface recombination. In the carrier statistical model adopted are the Fermidirac model and band gap narrowing (BGN) model. In addition, the current boundary condition of the electrode and the Dirichlet boundary condition between the electrode and the semiconductor are also considered. The simulation data under bias condition of $V_{ce} = 5.0$ V and $V_{be} = 1.0$ V are presented in Fig. 6, which shows the curve of photon-characteristic frequency $f_{t,opt}$ on collector current for SOI-based SiGe HPT and for Si-based SiGe HPT.

The Si-based SiGe HPT in Ref. [7] is also simulated by using this 2D simulation model. The maximum $f_{t,opt}$ of Si-based SiGe HPT is 957 MHz, which is a little larger than the measurement result (728 MHz) because some inevitable actual losses in measurement would not be considered in simulation. It is observed that the simulation data and measurement results are close to each other and therefore the 2D simulation model used in this work is reliable.

From Fig. 6, the result shows that at low current, the $f_{t,opt}$ of SOI-based SiGe HPT is evidently larger than that of Si-based SiGe HPT, with the maximum value of $f_{t,opt}$ reaching up to 24.51 GHz, which is 1.5 times greater than that of Si-based SiGe HPT. At high current, the $f_{t,opt}$ of SOI-based SiGe HPT is slightly greater than that of Si-based SiGe HPT.

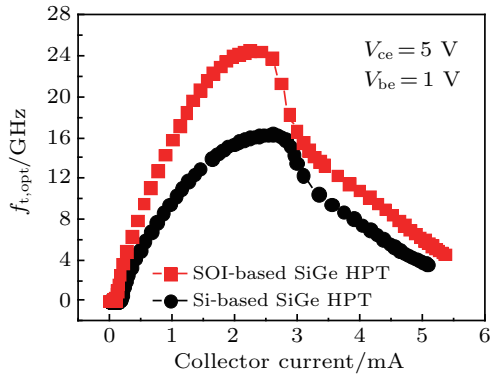


Fig. 6. Curve of $f_{t,opt}$ *versus* collector current for SOI-based SiGe HPT and for Si-based SiGe HPT.

At low current, by introducing BOX layer into Si-based SiGe HPT, as discussed above,the junction capacitance, including the collector–substrate capacitance C_{cs}, the base–collector capacitance C_{bc}, and the base–emitter capacitance C_{be}, decreases obviously. At the same time, the collector resistance almost keeps unchanged. Both will result in the decrease of total transfer time of carriers from emitter to collector. Thus, the value of $f_{t,opt}$ increases significantly. At high current, the advantage of BOX layer on base–collector capacitance and base–emitter capacitance becomes weak as shown in Figs. 4 and 5, the decrease of capacitance is not obvious, therefore, the $f_{t,opt}$ increases slightly at high current. Moreover, the BOX layer also isolates the slow carriers in the substrate and also benefits the improvement of $f_{t,opt}$.

The maximum optical cut-off frequency $f_{\beta,opt}$, also called the 3-dB bandwidth, is another important quality factor to characterize the high frequency characteristics of HPT, which can be expressed as[17]

$$f_{\beta,opt} = \frac{f_{t,opt}}{\beta_0}, \tag{3}$$

where β_0 is the common-emitter current amplification factor. Figure 7 shows the curves of the optical cut-off frequency *versus* collector current. It is observed that when the collector current is less than 2.75 mA, the $f_{\beta,opt}$ of SOI-based SiGe HPT is greater than that of Si-based SiGe HPT, and the maximum value of 3-dB bandwidth reaches up to 1.13 GHz, which is 1.18 times greater than that of Si-based SiGe HPT. It is clear that $f_{\beta,opt}$ is not proportional to $f_{t,opt}$ because amplification factor β_0 is also dependent on collector current. With the increase of collector current, the values of 3-dB bandwidth of two devices become almost the same, which is due to the difference in increasing speed and increasing magnitude between β_0 and $f_{t,opt}$.

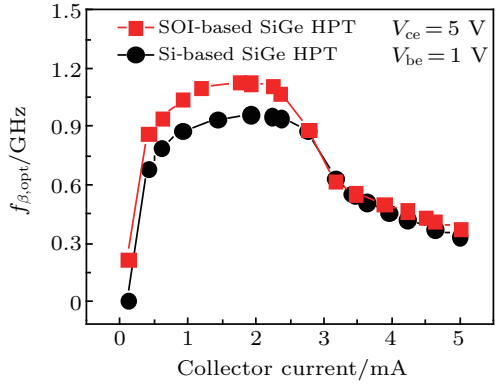


Fig. 7. Curve of $f_{\beta,opt}$ collector current for SOI-based SiGe HPT and for Si-based SiGe HPT.

As shown in Fig. 8, the increasing speed of $f_{t,opt}$ is fast than that of β_0 as current increases. So $f_{t,opt}$ reaches its maximum at a low current, while β_0 reaches its maximum at a high current. Furthermore, the magnitude of $f_{t,opt}$ is larger at a low current and the magnitude of β_0 is larger at a high current. Because of the difference in increasing speed and increasing magnitude between $f_{t,opt}$ and β_0 in the operation current range, the photon-characteristic frequency $f_{t,opt}$ has a dominated influence on $f_{\beta,opt}$ at low current, while at high current, the common-emitter current amplification factor β_0 has a greater influence on $f_{\beta,opt}$.

Therefore, in the case of low power, the SOI-based SiGe HPT has a higher 3-dB bandwidth, which benefits from the significant advantage of BOX layer on the device capacitance. In the case of high power, because of a large number of photogenerated carriers in emitter and base, even in collector, the advantage of BOX layer on frequency characteristic becomes less obvious, the 3-dB bandwidths of both devices are almost the same. Therefore, the technologies such as increasing the

gradient of Ge component in the base region or applying substrate bias voltage, may be considered to improve the working speed of the device in the future when it is used in high current areas.

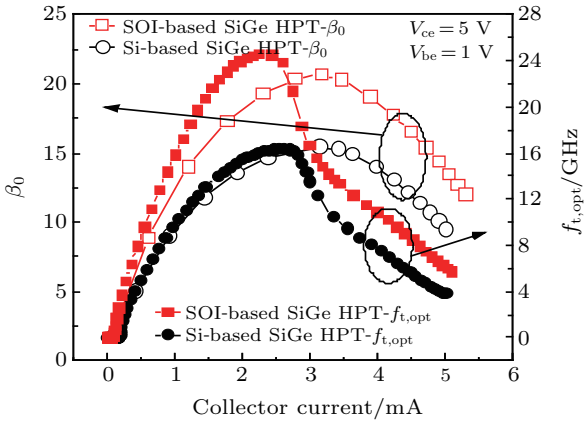


Fig. 8. Curves of β_0 and $f_{t,opt}$ *versus* collector current for SOI-based SiGe HPT and for Si-based SiGe HPT.

4. Conclusions

In this paper, the working speed of SOI-based SiGe HPT and Si-based SiGe HPT are analyzed. By introducing BOX layer into the Si-based SiGe HPT, the collector–substrate capacitance C_{cs} of the SOI-based SiGe HPT is always smaller than that of the Si-based SiGe HPT. Both the base–collector junction capacitance and the base–emitter junction capacitance decrease dramatically only at low current, but not so obviously at high current. Therefore, at low current, the photo-characteristic frequency $f_{t,opt}$ of SOI-based SiGe HPT is evidently greater than that of Si-based SiGe HPT. Specifically, the maximum value of the photon-characteristic frequency $f_{t,opt}$ reaches up to 24.51 GHz, which is 1.5 times greater than that of Si-based SiGe HPT. Moreover, the 3-dB bandwidth of SOI-based SiGe HPT is larger than that of Si-based SiGe HPT at low current, the maximum 3-dB bandwidth of SOI-based SiGe HPT reaches up to 1.13 GHz, which achieves 1.18 times greater than that of Si-based SiGe HPT. However, at high current,the values of 3-dB bandwidth of two devices are almost the same, which is due to the difference in increasing speed and increasing magnitude between $f_{t,opt}$ and β_0 in the operation current range. In summary, in the case of low power, the introduction of BOX layer exhibits dominant advantage in improving the working speed of SiGe HPT. In the case of high power, the advantage in improving the working speed of SiGe HPT becomes weak.

References

[1] Li H, Niu P J, Li J Y and Zhang Y 2006 *Elec-Optic. Technol. Appl.* **21** 18

[2] Li C, Xue C L, Liu Z, Cheng B W and Wang Q M 2014 *Chin. Phys. B* **23** 038507

[3] Ma P C, Sun X, Liu F M, Xue H Y, Sun Y, He H M, Li Z X and Cao L Q 2019 *Study Opt. Commun.* **3** 26

[4] Liu Y L, Yu C C, Lin K T, Yang T C, Wang E Y, Chen H L, Chen L C and Chen K H 2015 *ACS Nano* **9** 5093

[5] Rachel W and Mario P 2010 *Nat. Photon.* **4** 498

[6] Xue H Y, Xue C L, Cheng B W, Yu Y D and Wang Q M 2009 *Chin. Phys. B* **18** 2542

[7] Rosales M D, Schiellein J, Viana C, Polleux J L and Algani C 2012 *The 9th International Conference on Group I V Photonics* (GFP), August 29–31, 2012, San Diego, CA, USA, pp. 294–296

[8] Hsu K Y J and Liao B W C 2013 *IEEE International Conference of Electron Devices and Solid-state Circuits*, June 3–5, 2013, Hong Kong, China, pp. 1–12

[9] Tegegne Z G, Viana C, Rosales M, Polleux J L, Algani C, Grzeskowiak M and Richalot E 2015 *International Topical Meeting on Microwave Photonics* (MWP), October 26–29, 2015, Paphos, Cyprus, pp. 1–4

[10] Tegegne Z G, Viana C, Polleux J L, Grzeskowiak M and Richalot E 2016 *Silicon Photon. XI* February 15–17, 2016, San Francisco, CA, USA, 975219

[11] Tegegne Z G, Viana C, Rosales M D, Schiellein J, Polleux J L, Grzeskowiak M, Richalot E and Algani C 2017 *Int. J. Microw. Wirel. T.* **9** 17

[12] Varadharajaperumal M, Niu G F, Cressler J D, Reed R A and Marshall P W 2004 *IEEE Trans. Nucl. Sci.* **51** 3298

[13] Li C, Xue C L, Liu Z, Cong H, Cheng B W, Hu Z H, Guo X and Liu W M 2016 *Sci. Rep. UK* **6** 27743

[14] Sun D, Xie H Y, Liu R, Liu S, Wu J H and Zhang W R 2017 *Acta Photon. Sin.* **46** 49

[15] Liu S, Xie H Y, Sun D, Liu R, Wu J H and Zhang W R 2017 *J. Infrared Millim. Waves* **36** 594

[16] Jiang Z Y 2015 *Research on high frequency feature of InP-based uni-traveling-carrier double heterojunction phototransistor* (MS Dissertation) (Beijing: Beijing University of Technology) (in Chinese)

[17] Neamen D A 2013 *Smiconductor Physics and Devices Bssic Principles*, 4th edn. (Beijing: Publishing House of Electronics Industry) pp. 384–385